Exotic Searches with ATLAS

Rebecca Falla on behalf of the ATLAS Collaboration
University College London, UK

A summary was given of recent exotic searches with the ATLAS experiment using proton-proton collision data at $\sqrt{s} = 8$ TeV recorded in 2012 at the Large Hadron Collider.

1 Introduction

A summary was given of recent exotic searches with the ATLAS [1] experiment using proton-proton collision data at $\sqrt{s} = 8$ TeV recorded in 2012 at the Large Hadron Collider. Exotic searches are searches for new phenomena not including Supersymmetry. Unless explicitly stated, all analyses were performed on 20.3 fb^{-1} of data.

2 Long Lived Particle Searches

A summary of long-lived particle searches was presented, 95% CL exclusions were set on the lifetimes of many particles (see Figure 1).

3 Dark Matter

Results of a search for new phenomena in events with large missing transverse momentum and a Higgs boson decaying to two photons were reported [2]. The observed data are well described by the expected Standard Model (SM) backgrounds. Exclusion limits were presented for models of physics beyond the SM featuring dark matter candidates, for an example see Figure 2.

4 Vector Like Quarks

A search for pair production of vector-like quarks, both up-type (T) and down-type (B), as well as for four-top-quark production (see Figure 3), was presented [5]. Data were analysed in the lepton-plus-jets final state, characterised by an isolated electron or muon with high transverse momentum, large missing transverse momentum and multiple jets. Dedicated analyses were performed targeting three cases: a T quark with significant branching ratio to a W boson and a b-quark ($T\overline{T} \to Wb + X$), and both a T quark and a B quark with significant branching ratio to a Higgs boson and a third-generation quark ($T\overline{T} \to Ht + X$ and $B\overline{B} \to Hb + X$ respectively (see Figure 4 for examples)). No significant excess of events above the Standard Model expectation was observed, and 95% CL lower limits were derived on the masses of the vector-like T and B quarks under several branching ratio hypotheses assuming contributions from $T \to Wb$, Zt, Ht

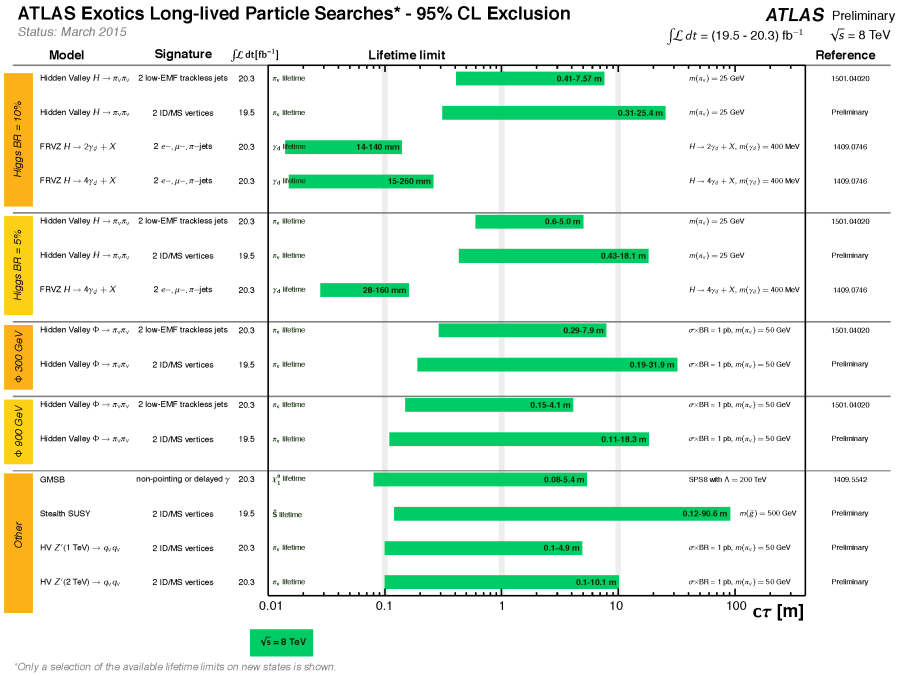

Figure 1: Reach in $c\tau$ of ATLAS searches for new phenomena. Only a representative selection of the available results is shown, (always up-to-date results are available here: https://twiki.cern.ch/twiki/bin/view/AtlasPublic/ExoticsPublicResults).

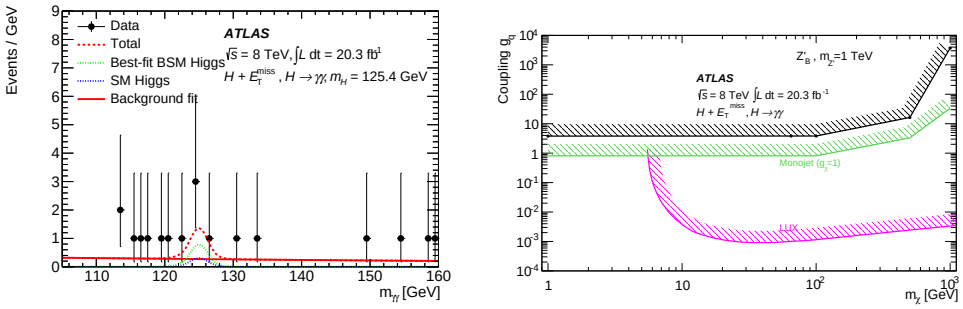

Figure 2:
(a) Distribution of the diphoton invariant mass $m_{\gamma\gamma}$. An unbinned maximum-likelihood fit to the spectrum is used to estimate the number of events from the continuum background and from $H \to \gamma\gamma$ decays; the individual components are shown as well as their sum.
(b) Limits on coupling parameters for simplified models with a heavy mediator with mass of 1 TeV. All constraint contours exclude larger couplings or mixing angles. Regions excluded due to perturbativity arguments are indicated; green and pink contours denote results from collider searches for monojet [3] searches, and the LUX Collaboration [4], respectively. Taken from Ref. [2]

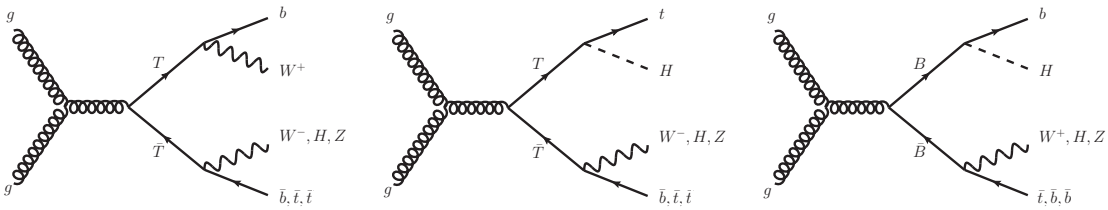

Figure 3: Representative leading-order Feynman diagrams for $T\overline{T}$ production probed by (a) the $T\overline{T} \to Wb + X$ search and (b) the $T\overline{T} \to Ht + X$ search, and (c) for $B\overline{B}$ production probed by the $B\overline{B} \to Hb + X$ search. Taken from Ref. [5]

and $B \to Wt$, Zb, Hb decays. The 95% CL observed lower limits on the T quark mass range between 715 GeV and 950 GeV for all possible values of the branching ratios into the three decay modes, and are the most stringent constraints to date (see Figure 5). Additionally, the most restrictive upper bounds on four-top-quark production were set in a number of new physics scenarios.

5 New Light Gauge Bosons

A search for Higgs bosons decaying to four leptons, either electrons or muons, via one or two light exotic gauge bosons Z_d, $H \to ZZ_d \to 4l$ or $H \to Z_dZ_d \to 4l$ was presented [6]. The observed data are well described by the Standard Model prediction (See Figure 6). Upper bounds on the branching ratio of $H \to ZZ_d \to 4l$ and on the kinetic mixing parameter between the Z_d and the Standard Model hypercharge gauge boson were set in the range $(1-9) \times 10^{-5}$ and $(4-17) \times 10^{-2}$ respectively, at 95% confidence level assuming the Standard Model branching ratio of $H \to ZZ^* \to 4l$, for Z_d masses between 15 and 55 GeV. Upper bounds on the effective mass mixing parameter between the Z and the Z_d were also set using the branching ratio limits in the $H \to ZZ_d \to 4l$ search, and are in the range $(1.5-8.7) \times 10^{-4}$ for $15 < m_{Z_d} < 35$ GeV. Upper bounds on the branching ratio of $H \to Z_dZ_d \to 4l$ and on Higgs portal coupling parameter, controlling the strength of the coupling of the Higgs boson to dark vector bosons, were set in the range $(2-3) \times 10^{-5}$ and $(1-10) \times 10^{-4}$ respectively, at 95% confidence level assuming the Standard Model Higgs boson production cross sections, for Z_d masses between 15 and 60 GeV (See Figure 7).

6 Heavy Lepton Resonances

A search for heavy leptons decaying to a Z boson and an electron or a muon was presented [7]. Three high-transverse-momentum electrons or muons were selected, with two of them required to be consistent with originating from a Z boson decay. No significant excess above Standard Model background predictions is observed (see Figure 8), and 95% confidence level limits on the production cross section of high-mass trilepton resonances were derived. The results were interpreted in the context of vector-like lepton and type-III seesaw models. For the vector-like lepton model, most heavy lepton mass values in the range 114-176 GeV were excluded. For the type-III seesaw model, most mass values in the range 100-468 GeV were excluded (See Figure 9).

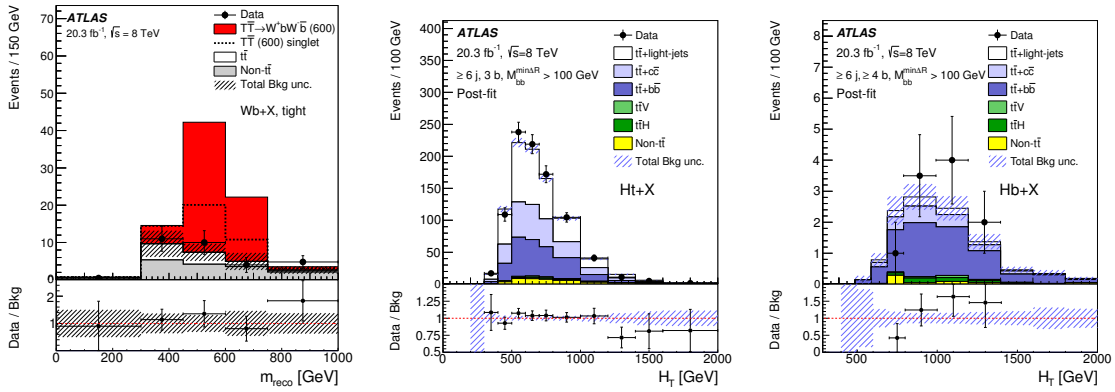

Figure 4:
(a) $T\overline{T} \to Wb + X$ search: distribution of the reconstructed heavy-quark mass (m_{reco}) after the tight selection, for the sum of W_{had}^{typeI} and W_{had}^{typeII} events. The data (solid black points) are compared to the SM prediction (stacked histograms). The total uncertainty on the background estimation is shown as a black hashed band. The expected contributions from a vector-like T quark with mass $m_T = 600$ GeV in two scenarios, BR($T \to Wb$) = 1 (red histogram) and singlet (dashed black histogram), are also shown stacked on top of the SM background.
(b) $T\overline{T} \to Ht + X$ search: comparison between data and prediction for the distribution of the scalar sum (H_T) of the transverse momenta of the lepton, the selected jets and the missing transverse momentum in one of the analysed channels after final selection: $\geq$ 6j, 3b, high $M_{bb}^{minΔR}$. The background prediction is shown after the fit to data under the background-only hypothesis.
(c) $B\overline{B} \to Hb + X$ search: comparison between data and prediction for the distribution of H_T in one of the analysed channels after final selection: $\geq$ 6j, $\geq$ 4b, high $M_{bb}^{minΔR}$. The background prediction is shown after the fit to data under the background-only hypothesis.
All plots: The contributions from backgrounds other than $t\bar{t}$ are combined into a single background source referred to as "Non-$t\bar{t}$". The last bin contains the overflow. The bottom panel displays the ratio of data to the total background prediction. The hashed area represents the total uncertainty on the background. Taken from Ref. [5]

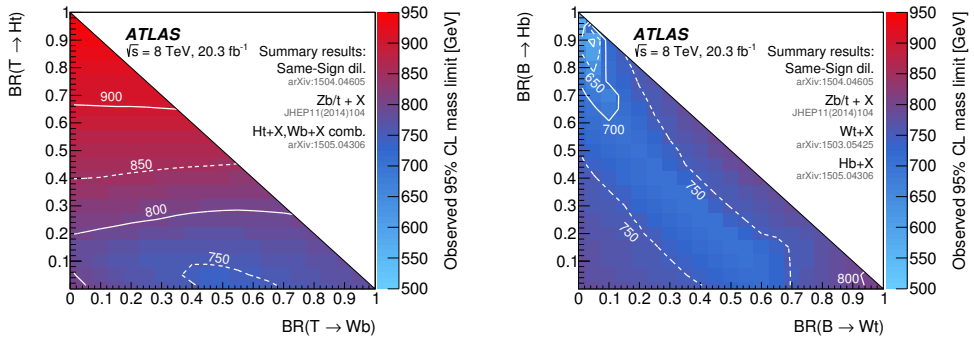

Figure 5: Summary of the most restrictive observed limit (95% CL) on the mass of the (a) T quark in the plane of BR($T \to Ht$) versus BR($T \to Wb$) and (b) B quark in the plane of BR($B \to Hb$) versus BR($B \to Wt$) from all ATLAS searches for $T\overline{T}$ or $B\overline{B}$ production, respectively. Contour lines are provided to guide the eye. Taken from Ref. [5]

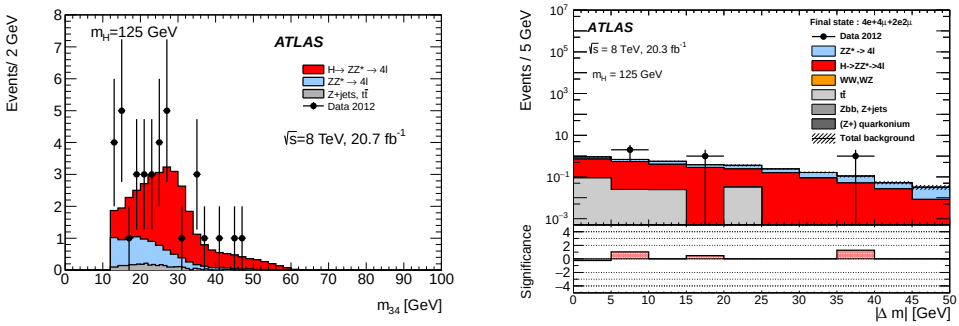

Figure 6:
(a)The distribution of the mass of the second lepton pair, m_{34}, of the data (filled circles with error bars) and the expected (pre-fit) backgrounds. The $H \to ZZ^* \to 4l$ expected (pre-fit) normalization, for a mass hypothesis of $m_H = 125$ GeV, is set by subtracting the expected contributions of the ZZ^*, Z+jets and $t\bar{t}$ backgrounds from the total number of observed $4l$ events in the data.
(b) Absolute mass difference, $\Delta m = |m_{12} - m_{34}|$ after the loose signal region requirements for the $4e$, 4μ and, $2e2\mu$ final states combined, for $m_H = 125$ GeV. The data is represented by the black dots, and the backgrounds are represented by the filled histograms. The shaded area shows both the statistical and systematic uncertainties. The bottom plots show the significance of the observed data events compared to the expected number of events from the backgrounds. Taken from Ref. [6]

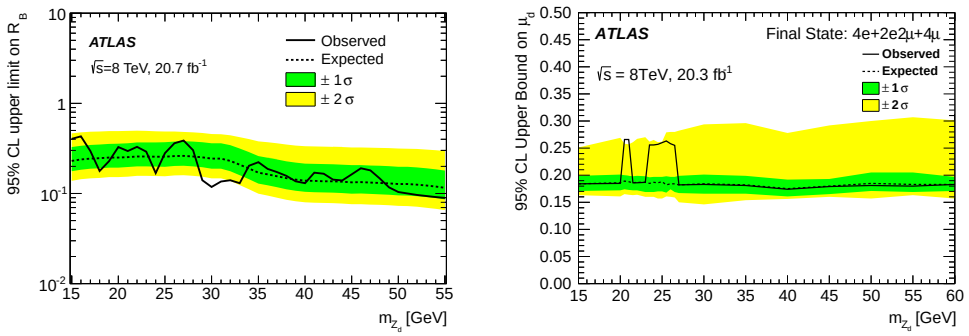

Figure 7:
(a) The 95% CL upper limits on the relative branching ratio, $R_B = \frac{BR(H \to ZZ_d \to 4l)}{BR(H \to 4l)}$ as a function of m_{Z_d}. The $\pm 1\sigma$ and $\pm 2\sigma$ expected exclusion regions are indicated in green and yellow, respectively.
(b) The 95% confidence level upper bound on the signal strength $\mu_d = \frac{\sigma \times BR(H \to Z_d Z_d \to 4l)}{[\sigma \times BR(H \to ZZ^* \to 4l)]_{SM}}$ of $H \to Z_d Z_d \to 4l$ in the combined $4e + 2e2\mu + 4\mu$ final state, for $m_H = 125$ GeV. The $\pm 1\sigma$ and $\pm 2\sigma$ expected exclusion regions are indicated in green and yellow, respectively. Taken from Ref. [6]

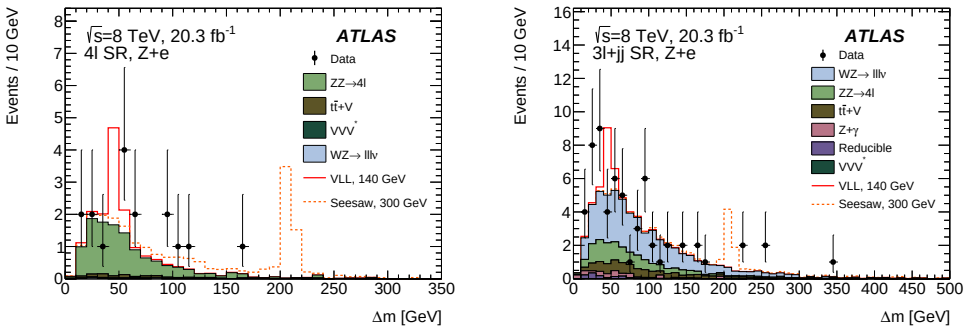

Figure 8: The $\Delta m = m_{3l} - m_{l^+l^-}$ distributions for the (a) $4l$ and (b) $3l + jj$ for the $Z + e$ channel. The observed data are shown as black points, while the pre-fit background expectations are shown in the coloured histograms. Also shown are examples for signal contributions for a 140 GeV $L^{\pm}$ in the VLL model and a 300 GeV $L^{\pm}$ in the type-III seesaw model. The error bars on the data points represent statistical uncertainties, and the shaded bands represent the systematic uncertainties on the background predictions. Taken from Ref. [7]

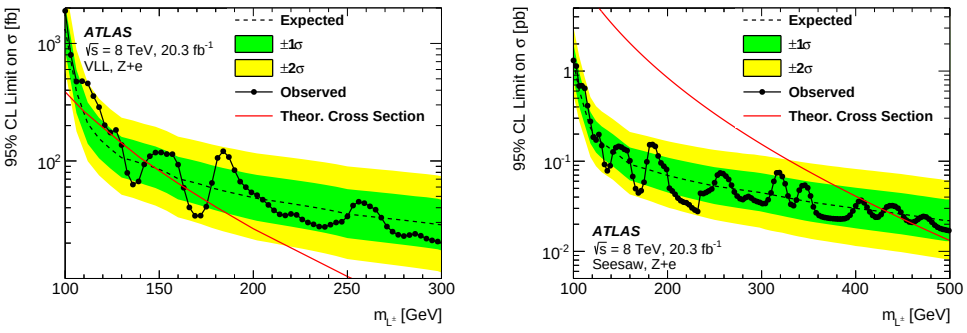

Figure 9: 95% CL upper limits on (a) the vector-like lepton cross section and (b) the type-III seesaw production cross section. The limits are assuming 100% branching fraction to e/ν_e. The solid line shows the observed limit. The dashed line shows the median expected limit for a background-only hypothesis, with green and yellow bands indicating the expected fluctuations at the $\pm 1\sigma$ and $\pm 2\sigma$ levels. The limit is evaluated in 3 GeV intervals. Taken from Ref. [7]

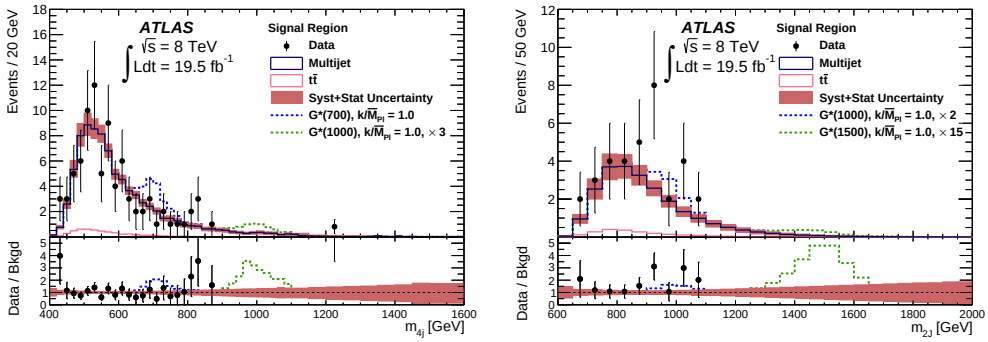

Figure 10:
(a) Distribution of the four-jet mass, m_{4j}, in the signal region of the resolved analysis for data (points) compared to the predicted background (solid histograms).
(b) Dijet mass distributions for data (points) as well as expected background (solid histograms) in the signal region of the boosted analysis.
The filled blocks represent the combined statistical and systematic uncertainty in the total background estimate. Simulated signal m_{4j} peaks for the bulk RS model with $\frac{k}{\bar{M}_{Pl}} = 1$ are shown as dashed lines. Taken from Ref. [8]

7 Higgs Boson Pair Production

A search for Higgs boson pair production $pp \to hh$ was performed with 19.5 fb^{-1} of data [8]. The decay products of each Higgs boson were reconstructed as a high-momentum $b\bar{b}$ system with either a pair of small-radius jets or a single large-radius jet, the latter exploiting jet substructure techniques and associated b-tagged track-jets. No evidence for resonant or non-resonant Higgs boson pair production was observed (See Figure 10). The data are interpreted in the context of the Randall–Sundrum model with a warped extra dimension as well as the two-Higgs-doublet model. An upper limit on the cross-section for $pp \to G^*_{KK} \to hh \to b\bar{b}b\bar{b}$ of 3.2 (2.3) fb was set for a Kaluza–Klein graviton G^*_{KK} mass of 1.0 (1.5) TeV, at the 95% confidence level (See Figure 11). The search for non-resonant Standard Model hh production set an observed 95% confidence level upper limit on the production cross-section $\sigma(pp \to hh \to b\bar{b}b\bar{b})$ of 202 fb, compared to a SM prediction of $\sigma(pp \to hh \to b\bar{b}b\bar{b}) = 3.6 \pm 0.5$ fb.

8 Top-Pair Resonances

A search for new particles that decay into top quark pairs was reported [9]. The lepton-plus-jets final state was used, where the top pair decays to $W^+bW^-\bar{b}$, with one W boson decaying leptonically and the other hadronically. The invariant mass spectrum of top quark pairs was examined for local excesses or deficits that are inconsistent with the Standard Model predictions (See Figure 12 (a)). No evidence for a top quark pair resonance was found, and 95% confidence-level limits on the production rate were determined for massive states in benchmark models. The upper limits on the cross-section times branching ratio of a narrow Z' boson decaying to top pairs range from 4.2 pb to 0.03 pb for resonance masses from 0.4 TeV to 3.0 TeV. A narrow leptophobic topcolour Z' boson with mass below 1.8 TeV was excluded (See Figure 12 (b)). Upper limits were set on the cross-section times branching ratio for a broad colour-octet resonance

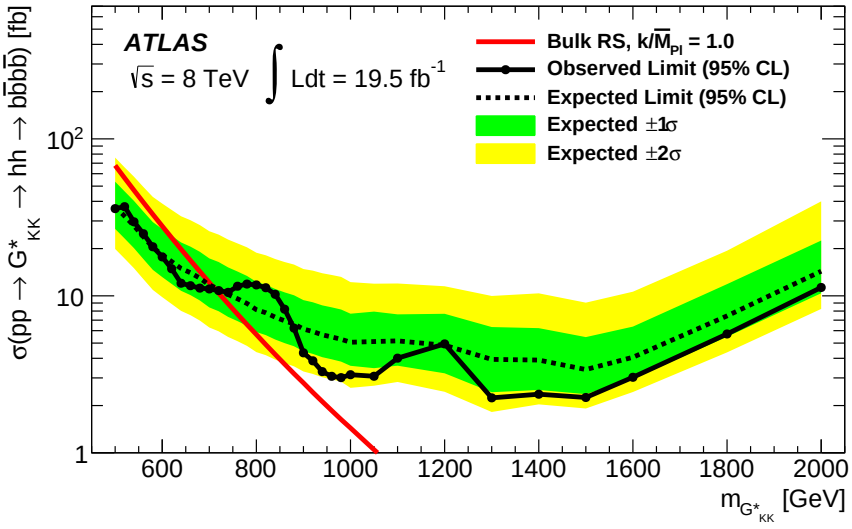

Figure 11: The combined expected and observed limit for $pp \to G^*_{KK} \to hh \to b\bar{b}b\bar{b}$ in the bulk RS model with $\frac{k}{\overline{M}_{Pl}} = 1$. The red curve shows the predicted cross-section as a function of resonance mass for the Graviton. Taken from Ref. [8]

with $\frac{\Gamma}{m} = 15\%$ decaying to $t\bar{t}$. These range from 2.5 pb to 0.03 pb for masses from 0.4 TeV to 3.0 TeV. A Kaluza-Klein excitation of the gluon in a Randall-Sundrum model was excluded for masses below 2.2 TeV.

9 High Mass Diboson Resonances

A search for narrow resonances decaying into WW, WZ, or ZZ boson pairs was presented [10]. Diboson resonances with masses in the range from 1.3 to 3.0 TeV were sought after using the invariant mass distribution of dijets where both jets were tagged as a boson jet, compatible with a highly boosted W or Z boson decaying to quarks, using jet mass and substructure properties. The largest deviation from a smoothly falling background in the observed dijet invariant mass distribution occured at around 2 TeV in the WZ channel (see Figure 13), with a global significance of 2.5 standard deviations. Exclusion limits at the 95% confidence level were set on the production cross section times branching ratio for the WZ final state of a new heavy gauge boson, W', and for the WW and ZZ final states of Kaluza–Klein excitations of the graviton in a bulk Randall–Sundrum model, as a function of the resonance mass. W' bosons with couplings predicted by the extended gauge model in the mass range from 1.3 to 1.5 TeV are excluded at 95% confidence level (see Figure 14).

10 Summary

Searches for exotic signatures with the ATLAS detector were presented. An overview of results of the ATLAS Exotics group is provided in Figure 15. Run 2 of the LHC has started at $\sqrt{s} = 13$ TeV and due to this increase in energy, along with a significant increase in integrated luminosity, we are expected to be even more sensitive to new physics.

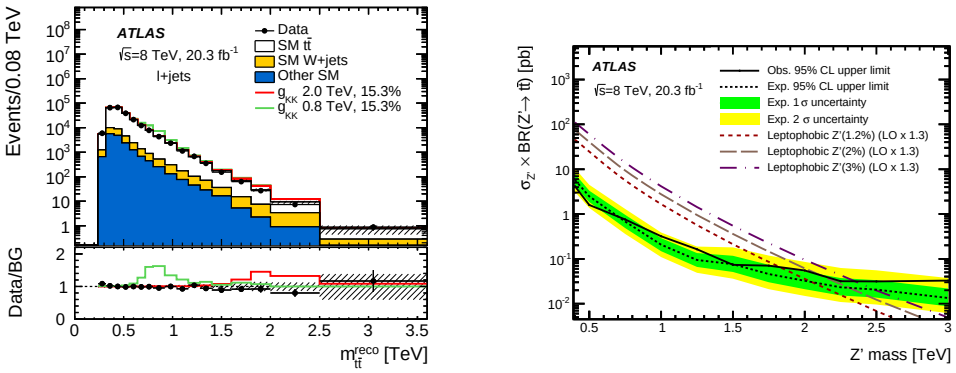

Figure 12:
(a) The m_{tt}^{reco} distributions, after the nuisance-parameter fit under the background-only hypothesis, summed over all 12 channels compared with data. The SM background components are shown as stacked histograms. The shaded areas indicate the total systematic uncertainties. The red (green) line shows the expected distribution for a hypothetical g_{KK} of mass 2.0 (0.8) TeV, width 15.3%.
(b) Observed and expected upper limits on the production cross-section times branching ratio to $t\bar{t}$ final states as a function of the mass of Topcolour-assisted-technicolour Z'_{TC2}. The expected limits are derived from nominal (pre-fit) background estimates. The theoretical predictions for the production cross-section times branching ratio at the corresponding masses is also shown. Taken from Ref. [9]

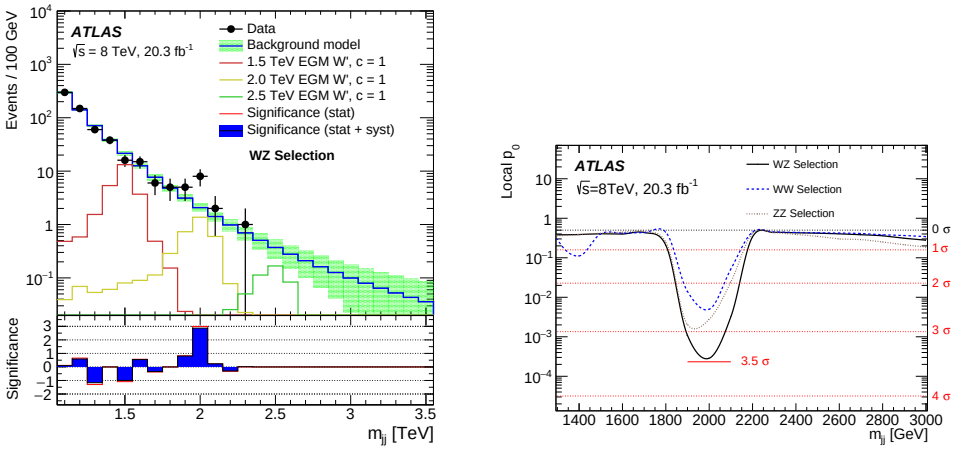

Figure 13:
(a) Background-only fits to the dijet mass (m_{jj}) distributions in data after tagging with the WZ selection. The significance shown in the inset for each bin is the difference between the data and the fit in units of the uncertainty on this difference. The significance with respect to the maximum-likelihood expectation is displayed in red, and the significance when taking the uncertainties on the fit parameters into account is shown in blue. The spectrum in this signal region is compared to the signals expected for an EGM W' with $m_{W'}$ = 1.5, 2.0, or 2.5 TeV.
(b) Local p_0 values for the WZ, WW and ZZ mass-window selections as a function of dijet mass. Since the WZ, WW and ZZ selections are not orthogonal, the observed p_0 are not independent between the three selections. Taken from Ref. [10]

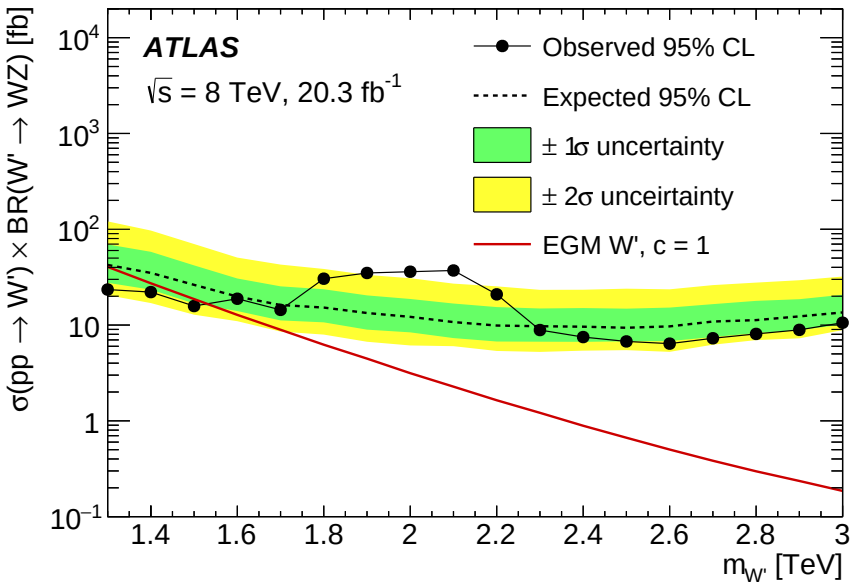

Figure 14: Upper limits, at 95% C.L., on the section times branching ratio limits for the WZ window selection as a function of $m_{W'}$. The solid red line displays the predicted cross section for the W' model as a function of the resonance mass. Taken from Ref. [10]

References

[1] ATLAS Collaboration, *JINST* **03**, S08003 (2008).

[2] ATLAS Collaboration, *Phys. Rev. Lett.* **115**, 131801 (2015).

[3] ATLAS Collaboration, *Phys. Lett.* **B705**, 294 (2013).

[4] LUX Collaboration, *Phys. Rev. Lett.* **112** 091303 (2014).

[5] ATLAS Collaboration, *JHEP* **08**, 105 (2015).

[6] ATLAS Collaboration, CERN-PH-EP-2015-111 (2015), arXiv:1505.07645 [hep-ex].

[7] ATLAS Collaboration, *JHEP* **09**, 108 (2015).

[8] ATLAS Collaboration, *Eur. Phys. J.* **C75**, 412 (2015).

[9] ATLAS Collaboration, *JHEP* **08**, 148 (2015).

[10] ATLAS Collaboration, CERN-PH-EP-2015-115 (2015), arXiv:1506.00962 [hep-ex].

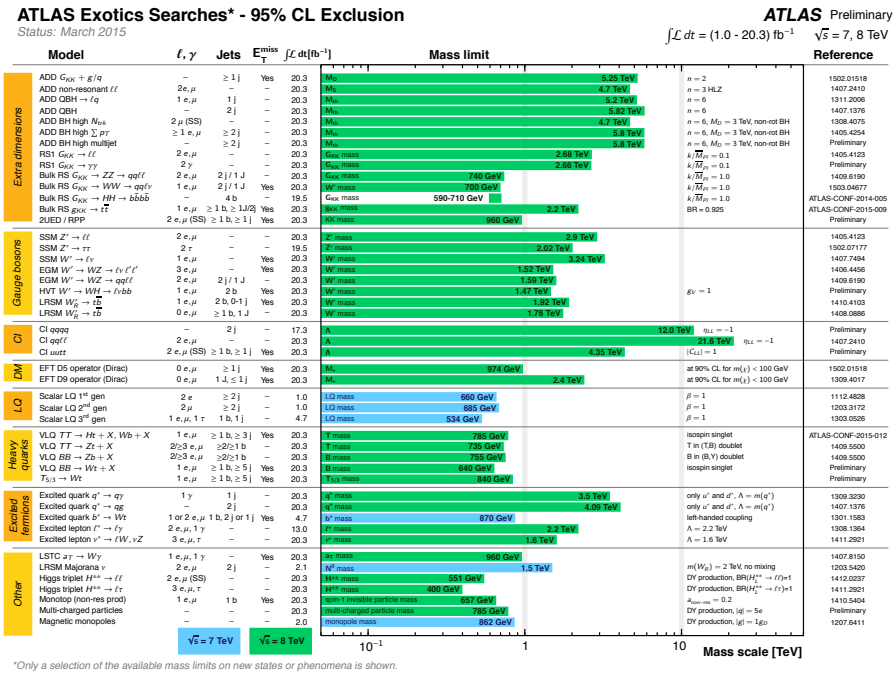

Figure 15: Reach of ATLAS searches for new phenomena other than Supersymmetry. Only a representative selection of the available results is shown. Blue (green) bands indicate 7 TeV (8 TeV) data results, (always up-to-date results are available here: https://twiki.cern.ch/twiki/bin/view/ AtlasPublic/ExoticsPublicResults).